

Reply to the reviewer's #1 comments

Manuscript title: “Lidar observation of the 2011 Puyehue-Cordón Caulle volcanic aerosols at Lauder, New Zealand”

MS No.: acp-2014-14

We thank reviewers for reading our manuscript carefully and for giving useful comments. We extensively revised our manuscript along the reviewer's comments, and below are our responses to them. Reviewer's comments are shown in italic and our responses are continued after them. The page and line numbers refer to those published in Atmos. Chem. Phys. Discuss.

p. 13466 l. 21: Please shortly introduce the volcanic explosivity index to readers who may not be familiar with this. Also indicate how the index is related to injection height.

We added the follow paragraph in page13466 line21.

“The VEI was developed as a simple and semi-quantitative scheme for estimating the magnitude of historic eruptions by Newhall and Self (1982). Eruptions are assigned to a VEI on a scale of 0 to 8, using the criteria such as the volume of ejecta, column height and qualitative of the eruption. Especially, the volume of ejecta and the column height are important.”

p. 13467 l. 11: It might be worth mentioning, that also windshield abrasion and reduction of visibility and sight are volcanic hazards to aviation.

We added the sentence in page13467 line13.

“The volcanic hazards for aircraft have been recognized that are the stop of aviation engines, reduction of visibility and the damage to windshield due to volcanic ash (Bernard, 1990).”

Additional reference: The Injection of Sulfuric Acid Aerosols in the Stratosphere by the El Chichon Volcano and its Related Hazards to the International Air Traffic, Bernard, 1990.

p. 13468 ll. 1ff.: Derivation of the tropopause height is a key element of this study. Nevertheless the authors do not explain how the tropopause height is determined (e.g. by temperature minimum, by wind speed maximum, by potential temperature slope, by potential vorticity. There are a lot of definitions of "tropopause" out there). It would be good to add a short paragraph on this method here.

We added the sentence in page13468 line4.

“We use the tropopause height as the lowest level at which the temperature lapse rate is less than 2 K/km for higher levels within 2 km defined by the WMO (WMO 1957).”

Additional reference: WMO, 1957: Definition of the tropopause. WMO Bull., 6, 136.

p. 13469 l.14: I agree with the value of the lidar ratio, nevertheless the authors are encouraged to reference section 3.3 here in order to reduce confusion for the reader.

We corrected in manuscript. (We added sentence in page13469 line14.)

“We assumed the lidar ratio S to be 50 sr at both 532 and 1064 nm in this study from some previous studies (see section 3.3).”

p. 13469 ll. 21ff.: Which radiative transfer model has been used for calculating the molecular backscatter coefficient?

We didn't use the radiative transfer model.

We need the molecular backscattering coefficient and the extinction coefficient to calculate the aerosol backscattering coefficient from lidar signals. The molecular backscattering (Rayleigh scattering) coefficient and the extinction coefficient are taken from Bucholtz et al. (1995) using the atmospheric density profiles obtained from radiosonde data launched at Invercargill.

p. 13470 ll. 4f.: A reference to non-spherical particles being related to positive delta would be appreciated.

We corrected our manuscript and added references.

Because backscattering by spherical particles does not change the laser polarization, $\delta = 0$ for spherical particle. The depolarization ratio is sensitive to the non-spherical particles. When $\delta > 0$, the scattering by non-spherical particles is recognized (Sassen 1991).

Additional reference: Sassen, K.: The polarization lidar technique for cloud research: A review and current assessment, Bull. Amer. Meteor. Soc., 72, 1848-1866, 1991.

p. 13472 ll. 16ff.: Do the authors have any explanation, why delta is significantly lower for the Eyjafjalla case compared to PCC? Might the reason be the different mineralogical composition (mid-ocean ridge volcano versus subduction zone volcano), the amount of ejected SO₂/H₂SO₄, or anything else?

We cannot explain the reason for difference of kind of ejected components from two volcanoes, the Eyjafjallajökull and the PCCVC eruption. The significant difference in δ might be due to the difference in distance between the volcano and the observation site, or the difference of the amount of each volcanic ejecta.

eq. (6): It would be good to shortly explain which assumptions go into this equation (as it is a strong simplification of the radiative transfer problem).

Uchino et al. (1983) did not use assumptions and simplifications for deriving Eq.(6) from Lidar equation.(Lidar chapter1 .p20)

Reference: Weitkamp, C. (Ed.): Lidar -Range-Resolved Optical Remote Sensing of the Atmosphere-, Springer Series in Optical Sciences, Vol. 102, chapter1 .p20, 2005.

p. 13474 l. 1: A value of 13% AOD difference is quite a close coincidence given the uncertainties and simplifications. How does it relate of the lidar ratios discussed above (i.e. could the difference be explained by the spread of potential lidar ratios)?

A value of 13% is the difference between the AOD derived by IBC and the AOD derived by Eq.(6). Whereas the AOD derived by IBC have the error depending on uncertainty of lidar ratio, the AOD derived by Eq.(6) does not depend on the lidar ratio, and its value has 0.08 in analysis error, that is the range of AOD=0.44-0.6. Hence, it is presumed that 13% error contains both the above analysis error and the uncertainty of lidar ratio.

p. 13474 l.2: How do the authors get the uncertainty of about 20% for the AOD from IBC? A short explanation would help understanding these numbers.

We corrected and added our manuscript in page13474 line1-2.

“; this AOD value is 13 % larger than the AOD derived from the IBC and S. The values of AOD derived by Eq.(6) are 0.17 and 0.12 on 24 June and 6 June, respectively. On average, the AOD derived by IBC was about 20 % smaller than AOD derived by Eq.(6). If the lidar ratio is assumed to be 60 sr, AOD will be consistent each other.”

Reply to the reviewer #2's comments

Manuscript title: “Lidar observation of the 2011 Puyehue-Cordón Caulle volcanic aerosols at Lauder, New Zealand”

MS No.: acp-2014-14

We thank reviewers for reading our manuscript carefully and for giving useful comments. We extensively revised our manuscript along the reviewer's comments, and below are our responses to them. Reviewer's comments are shown in italic and our responses are continued after them. The page and line numbers refer to those published in Atmos. Chem. Phys. Discuss.

Abstract:

Line 5-6: As this study seems not the main focus of the paper, it should not be stated here.

We deleted it and added a following sentence before the final sentence.

“The purpose of our study is to quantify the influence of the volcanic ejections from large eruption, and we use the data from the ground-based lidar observation.”

Line 8: The authors should already indicate here that they consider linear depolarization.

The total depolarization ratio that we derived from lidar signals was the linear depolarization ratio.

Line 9: Is this the volume or particle depolarization?

Yes, it is the volume depolarization ratio

Section1:

Page 13466, line 23-24: Give a reference for that statement.

We added a reference. : Robock (2000)

Page 13467, line 14-16: The references do not only consider small particles but also large volcanic ash particles.

We added the follow sentence in page13467 line14-15.

“The ash plumes from volcano were transported to central Europe, and the heights of these ash layers were low enough to deposit on surface after about 6 days from the eruption.”

Page 13467, line 17-19: Give the explosivity index

We added the VEI in our manuscript.

The VEI of the PCCV eruption in 2011 was about 3. (Dzierma. and Wehrmann, 2012)
Additional reference: Dzierma, Y. and Wehrmann H.: On the likelihood of future eruptions in the Chilean Southern Volcanic Zone: interpreting the past century's eruption record based on statistical analyses, *Andean Geology*, 39, 3, 380-393, doi: 10.5027/andgeoV39n3-a02, 2012.

Section 2:

Page 13469, line 14: Give an explanation and reference for the assumed lidar ratio.

We added a following sentence.

“We assumed the lidar ratio S to be 50 sr at both 532 and 1064 nm in this study from some previous studies (see section 3.3).”

Section 3:

The authors assume aerosol free regions at about 30 km altitude and found low R values (about 1.09) in the stratosphere (except in the volcanic aerosol layer) indicating aerosol free regions. However above the volcanic aerosol layer the total depolarization ratio (Fig. 1, 4, 6) is about 2%. What is the reason why the total depolarization differs from the molecular depolarization ratio assumed in this aerosol free regions?

The value of 0.37 is theoretical value, and has the difference from the measured value which is resulting from the lidar system error.

We can estimate this system error using method of Sakai et al. (2003).

We calculated about 0.65% of lidar system error. The measured depolarization was about 1.0-1.2% from Fig. 6, and this value was coincided with a fact that when the theoretical value is 0.37 %, the lidar system error is about 0.65%. According to Sakai et al. (2003), this error value is the ratio of the intensity of the perpendicular component to the total intensity of the outgoing laser beam after transmission from the lidar.

We added the sentences of “The measured δ was about 1.0-1.2 % at altitudes higher than about 15 km (see Figs. 4 and 6), and this indicates that δ is sum of δ_m (0.37 %) and the lidar system error (about 0.65 %) where there were no aerosols. We estimated δ_p taking into accounting of this lidar system error (Sakai et al., 2003). When R is close to 1.0, δ_p has a larger error. For example, when $R=1.05$ and $\delta_p = 8$ %, the error of δ_p is larger than 20 %.” in the section 3.2.

The particle depolarization ratio shows no constant value in the volcanic aerosol layer. Do the authors expect vertical variability of the microphysical parameters inside the volcanic aerosol layer (page 13472, line 25-28)? How could that be explained?

We could not confirm the descending of aerosol layer from lidar data.

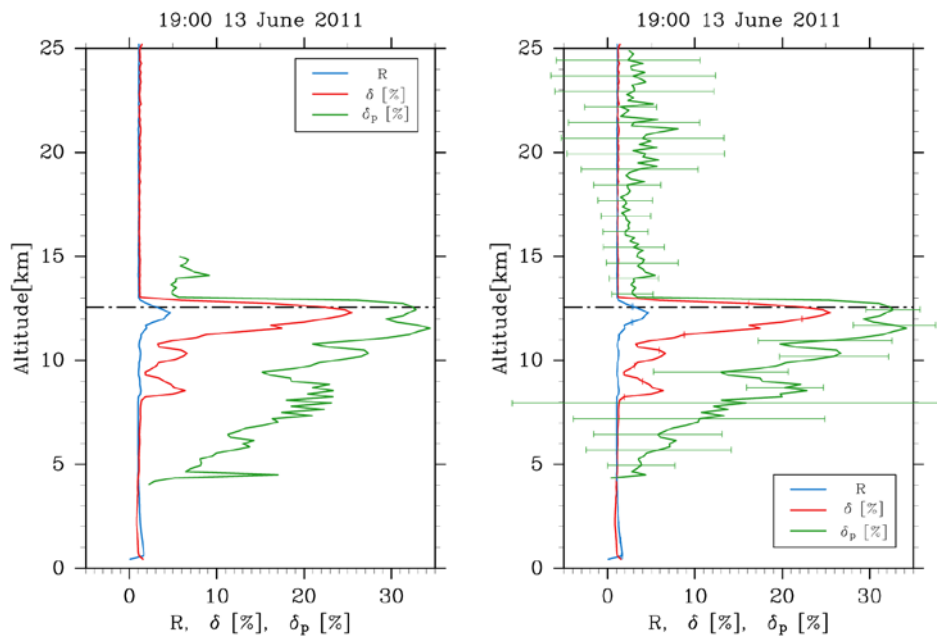
The non-uniform particle depolarization ratio shows that the different proportion of non-spherical particles in the volcanic aerosol layer is in each different height. We could not consider the vertical variability of the microphysical parameters inside the volcanic aerosol layer from only the lidar data.

What is the lowest R value for reliable analysis of the particle depolarization ratio?

The authors should give a comprehensive error analysis of the retrieved properties, especially of the particle depolarization ratio, to avoid drawing wrong conclusion of the retrieved results.

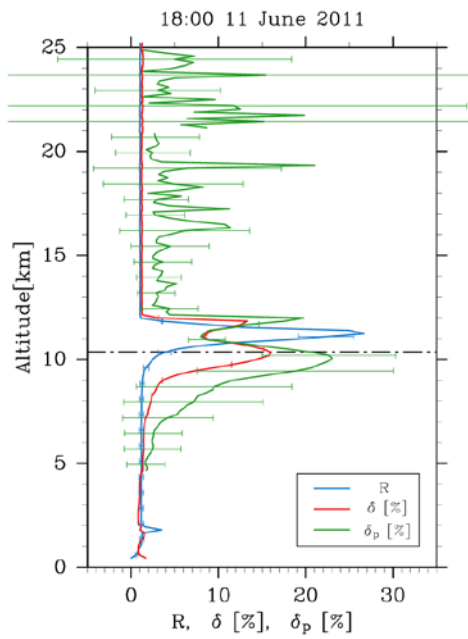
We showed the error of δ_p in each different height in new Fig.6(a).

From this figure, we confirmed that the values of δ_p higher than altitude 15 km and lower than altitude 8 km ($R \cong 1.0$) have very larger error. (The error of R and δ are sufficiently smaller than that of δ_p , see right panel.)

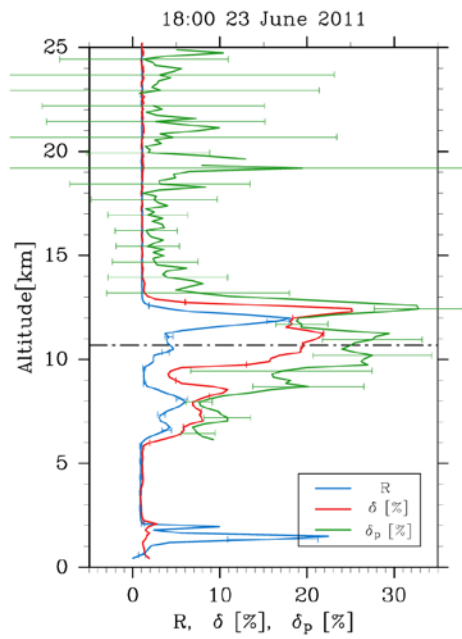


Also we show plots in Figures 4(a)-(c) with the error of δ_p below.

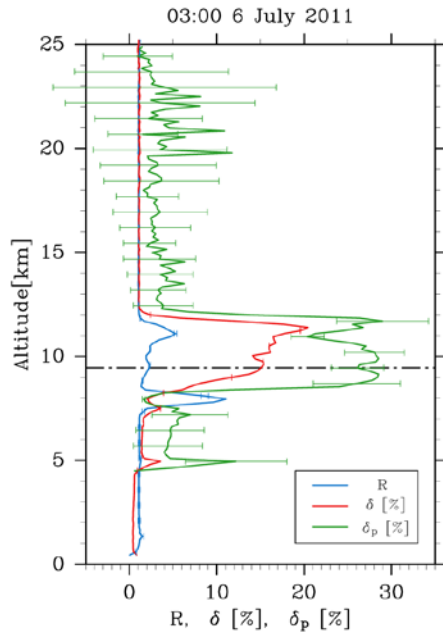
(a)



(b)



(c)



We corrected δ_p and replaced Figs. 4(a) - (c) and Fig. 6(a).

Lidar observation of the 2011 Puyehue-Cordón Caulle volcanic aerosols at Lauder, New Zealand

K. Nakamae¹, O. Uchino¹, I. Morino¹, B Liley², T. Sakai³, T. Nagai³, T. Yokota¹

[1]{National Institute for Environmental Studies, Tsukuba, Japan}

[2]{National Institute of Water and Atmospheric Research, Lauder, New Zealand}

[3]{Meteorological Research Institute, Tsukuba, Japan}

Correspondence to: K. Nakamae (nakamae.kumi@nies.go.jp)

Abstract

On 4 June, 2011, the Puyehue-Cordón Caulle volcanic complex (40.6°S, 72.1°W) in Chile erupted violently and injected volcanic aerosols into the atmosphere. For the safety of civil aviation, continuous lidar observations were made at Lauder, New Zealand (45.0°S, 169.7°E), from 11 June through 6 July 2011. [The purpose of our study is to quantify the influence of the volcanic ejections from large eruption, and we use the data from the ground-based lidar observation.](#) We analyzed lidar data at a wavelength of 532 nm and derived the backscattering ratio and depolarization ratio profiles. During June and July, within the altitude range of 10–15 km, the volcanic aerosols had high depolarization ratios (20–35%), an indication of non-spherical volcanic ash particles. The time series of the backscattering ratio during continuous observations had three peaks occurring at about 12 day intervals: 26.7 at 11.2 km on 11 June, 18.1 at 12.0 km on 23 June, and 5.3 at 11.1 km on 6 July. The optical depth of the volcanic aerosols was 0.45 on 11 June, when the continuous lidar observation started, 0.31 on 23 June, and 0.12 on 6 July. The depolarization ratio values remained high up to a month after the eruption and the small wavelength exponent calculated from the backscattering coefficients at 532 nm and 1064 nm suggest that a major constituent of the volcanic aerosols was large, non-spherical particles. The presence of volcanic ash in the stratosphere might affect the error in

1 the Greenhouse gases Observing SATellite (GOSAT) XCO₂ retrievals using the 1.6 μm band.
2 We briefly discuss the influence of the increased aerosols on the GOSAT products.

4 **1 Introduction**

5 The eruptions with a volcanic explosivity index (VEI) larger than 4 to 5 are generally
6 expected to inject volcanic aerosols into the stratosphere (Newhall and Self, 1982; Deshler,
7 2008; Vernier et al., 2011; Trickl et al., 2013). The VEI was developed as a simple and semi-
8 quantitative scheme for estimating the magnitude of historic eruptions by Newhall and Self
9 (1982). Eruptions are assigned to a VEI on a scale of 0 to 8, using the criteria such as the
10 volume of ejecta, column height and qualitative of the eruption. Especially, the volume of
11 ejecta and the column height are important. Volcanic aerosol particles larger than 10 μm
12 injected into the stratosphere settle rapidly, so their climatic effects can generally be neglected
13 (Robock, 2000). Volcanic ash is known to affect tropospheric cloud phases by acting as ice
14 nuclei (Durant et al., 2008; Latham et al., 2011). In contrast, when a large amount of sulfur
15 dioxide is injected into the stratosphere, it is converted to sulfuric acid particles within several
16 weeks (Zhao et al., 1995). The Mt. Pinatubo volcano (Philippines, 15.1°N; 120.35°E) erupted
17 on 15 June, 1991 and stratospheric injection of about 20 Mt of SO₂ was detected by the Total
18 Ozone Mapping Spectrometer (Bluth et al., 1992). The SO₂ is oxidized to sulfuric acid vapor
19 from which sulfuric acid particles are produced by homogeneous nucleation (Wu et al., 1994).
20 These particles are long-lived in the stratosphere (Uchino et al, 1995; Nagai et al., 2010),
21 depending on the latitude and altitude of injection, and significantly affect the global climate
22 and radiation budget and the ozone layer (Minnis et al, 1993; McCormick et al., 1995;
23 Alados-Arboledas et al., 1997; Robock 2000; Solomon et al., 2011).

24 Large amounts of volcanic ash in the atmosphere can damage aircraft engines and raise flight
25 safety concerns; as a result they can have significant consequences for air traffic. The volcanic
26 hazards for aircraft have been recognized that are the stop of aviation engines, reduction of
27 visibility and the damage to windshield due to volcanic ash (Bernard, 1990). For example, the
28 ash plume from the eruption of the Eyjafjallajökull volcano (63.63°N, 19.62°W, Iceland) on
29 14 April 2010 disrupted air traffic over Europe. The ash plumes from volcano were
30 transported to central Europe, and the heights of these ash layers were low enough to deposit
31 on surface after about 6 days from the eruption. The small particles and trace gases such as

1 SO₂ from this eruption were transported over long distances (Tesche et al., 2010; Ansmann et.
2 al., 2010; Wiegner et al., 2012).

3 On 4 June 2011, the Puyehue-Cordón Caulle Volcanic Complex (hereafter PCCVC; 40.59°S,
4 72.11°W) in Chile erupted and injected large amounts of volcanic ash particles into the
5 atmosphere (VEI=3) (Dzierma and Wehrmann, 2012). This volcanic complex had previously
6 erupted in May 1960 (Lara et al., 2004; Raga et al., 2013). The volcanic aerosol plumes
7 travelled eastward from Chile via the prevailing westerlies and passed over New Zealand
8 (Klüser et al., 2013). Because the Volcanic Ash Advisory Center (VAAC) in Wellington had
9 forecast that a large volcanic aerosol plume would reach New Zealand, we performed
10 continuous observations of volcanic aerosols with lidar at Lauder (45.04°S, 169.68°E), New
11 Zealand, and provided the observational data to the VAAC for the safety of civil aviation. The
12 aerosol lidar system at Lauder is a two-wavelength polarization lidar. In this study, we used
13 continuous lidar observational data observed at Lauder from 11 June through 6 July 2011. We
14 retrieved the backscattering ratios at 532 nm and 1064 nm and the depolarization ratio at 532
15 nm, and we calculated the ratio of the backscattering coefficients at 532 nm and 1064 nm.
16 For meteorological data and derivation of the tropopause height required for the lidar data
17 analysis, we used the twice-daily radiosonde data observed at Invercargill (46.42°S,
18 168.33°W), 186 km south-west of Lauder. [We use the tropopause height as the lowest level at](#)
19 [which the temperature lapse rate is less than 2 K/km for higher levels within 2 km defined by](#)
20 [the WMO \(WMO, 1957\).](#)

21 In the next section, we describe the lidar system at Lauder. In section 3, we present the
22 analysis and results and we discuss the backscatter wavelength dependence in section 4.

23

24 **2 Lidar system and data analysis**

25 Lidar measurement of stratospheric aerosols at Lauder was started in November 1992, owing
26 to interest in the then-recent eruption of Mt Pinatubo (Uchino et al., 1995) and as a

1 component of the nascent Network for the Detection of Stratospheric Change, subsequently
2 the Network for the Detection of Atmospheric Composition Change. Though that system had
3 only a single detector (532 nm), some depolarization measurements were made starting in
4 November 1995. The system operated reliably for 17 years and recorded the decline of the
5 Pinatubo aerosol to a minimum in the late 1990s (Nagai et al. 2010), followed by an increase
6 in stratospheric aerosols by other volcanoes (Vernier et al., 2011; Uchino et al., 2012). In
7 February 2009 this lidar system was updated for both daytime and night-time observations of
8 aerosols and clouds for Greenhouse gases Observing SATellite (GOSAT) product validation
9 (Nagai et al., 2009). The updated system is a two-wavelength polarization lidar. In this study,
10 we use lidar data obtained by continuous measurements from 11 June 2011 to 6 July 2011,
11 with measurements made before and after this period for GOSAT product validation. The
12 main lidar specifications are summarized in Table 1. The light source of the lidar system is a
13 Nd:YAG laser with a second-harmonic generator: the laser thus operates at two wavelengths,
14 532 nm and 1064 nm. The pulse repetition rate is 10 Hz, and the transmitted energy is 150 mJ
15 per pulse. The receiving telescope has a diameter of 30.5 cm. The signal at 1064 nm is
16 detected with an analogue-mode avalanche photo diode (APD), and two polarization
17 components of the signals at 532 nm are detected with three photomultiplier tubes (PMTs)
18 from the near surface to a high altitude of ~40 km.

19 In this study, we used the Fernald method (Fernald, 1984), in which the lidar equation for
20 retrieving vertical profiles of the aerosol backscatter coefficients from lidar signal intensity is
21 solved by assuming an extinction-to-backscatter ratio (lidar ratio). We also assumed that there
22 was no aerosol in the upper atmosphere at around 30 km, and used the value from that altitude
23 as a reference value by which to normalize the rest of the profile. The lidar ratio is an
24 important parameter for obtaining profiles of the particle extinction coefficient from lidar
25 signals to use for iterative correction of the backscatter profile. The lidar ratio S is defined as
26 the ratio of the extinction coefficient α to the backscattering coefficient β :

$$27 \quad S = \frac{\alpha}{\beta}. \quad (1)$$

28 We assumed S to be 50 sr at both 532 and 1064 nm in this study from some previous studies
29 (see section 3.3). The lidar ratio depends on particle properties such as their size distribution
30 and shape. The backscattering ratio R is defined as follows:

$$31 \quad R = (\beta_A + \beta_M) / \beta_M, \quad (2)$$

1 where β_A is the aerosol backscattering coefficient and β_M is the molecular backscattering
2 coefficient. For a pure Rayleigh atmosphere $R = 1.0$, and the backscatter signal from aerosols
3 increases as R becomes larger than 1.0. The molecular backscattering coefficient β_M was
4 calculated by using the atmospheric density profiles obtained from radiosonde data launched
5 at Invercargill (46.45°S, 168.33°W) (Bucholtz et al., 1995).

6 The lidar transmits linearly polarized light at 532 nm and records the backscattering intensity
7 with parallel P_{\parallel} and perpendicular P_{\perp} polarization to the transmitted polarization. The total
8 depolarization ratio δ is defined as

$$9 \quad \delta = \frac{P_{\perp}}{(P_{\parallel} + P_{\perp})} \times 100 \%. \quad (3)$$

10 Because backscattering by spherical particles does not change the laser polarization, $\delta = 0$ for
11 spherical particle. The depolarization ratio is sensitive to the non-spherical particles. When
12 $\delta > 0$, the scattering by non-spherical particles is recognized (Sassen,1991) .

13

14 **3 Results**

15 **3.1 Comparisons of aerosol vertical profiles before and after the eruption**

16 Figure 1 shows the vertical profiles of R and δ before and after the PCCVC eruption. The first
17 aerosol plume from the PCCVC eruption on 4 June 2011 was observed by lidar at Lauder at
18 midnight on 11/12 June. The volcanic aerosol peak was located above the tropopause
19 (10.35km) on 11 June. The peak R value at 532 nm was 26.7 at 11.23 km, and the peak δ
20 value at 532 nm was 16.0 % at 10.3 km. The maximum value of R on 28 May (before the
21 eruption) around 7 km was due to tropospheric aerosols; the maximum value of R in the
22 stratosphere was 1.09 at 16.03 km.

23 The integrated backscattering coefficient (IBC) is defined by Eq. (4)

$$24 \quad IBC = \int_{z_{tr}}^{z_{top}} \beta_A dz . \quad (4)$$

25 We calculated IBC from the tropopause height z_{tr} to z_{top} , taking $z_{top} = 30$ km.

26 IBC represents the amount of stratospheric aerosol loading at a given location. IBC was
27 $2.2 \times 10^{-4} \text{ sr}^{-1}$ on 28 May; this value is slightly larger than the stratospheric background
28 value of $1.42 \times 10^{-4} \text{ sr}^{-1}$ (Nagai et al., 2010). On 11 June, after the eruption, IBC was

1 $8.5 \times 10^{-3} \text{ sr}^{-1}$; this value indicates that the PCCVC aerosols had reached the stratosphere
2 over Lauder. We calculated forward trajectories to confirm that the observed profile peaks
3 represented layers of volcanic aerosols derived from the PCCVC eruption. We calculated 10
4 day isentropic forward trajectories of air parcels by using the METEX (Meteorological Data
5 Explorer) software package, which is provided by the National Institute for Environmental
6 Studies and driven by NCEP/NCAR Reanalysis Data (Kalnay et al., 1996) 4 times daily (Fig.
7 2).

8 The initial points of 15 air parcels at 11 km altitude were located in a $1^\circ \times 1^\circ$
9 latitude/longitude box centered at the PCCVC eruption and released at 17 UTC on 4 June.
10 The calculations showed that the air parcels leaving the volcano on 4 June 2011 reached
11 Lauder in the early morning of 12 June. The calculations also showed that 43 % of all air
12 parcels reached the vicinity of Lauder, and the volcanic aerosol plume from the PCCVC
13 eruption remained near the tropopause level in the mid-latitudes of the Southern Hemisphere.
14 These results agree with the findings of Klüser et al. (2013), who used backward trajectory
15 calculations and observations of the Infrared Atmospheric Sounding Interferometer (IASI) on
16 board the MetOp satellite to determine the evolution of the ash plume around the Southern
17 Hemisphere.

18 **3.2 Vertical profiles of the backscattering ratio and the depolarization ratio**

19 Vertical and temporal cross sections of the backscattering ratio and depolarization ratio at 532
20 nm over Lauder are presented in Fig. 3. Volcanic aerosol layers with a large backscattering
21 ratio above the tropopause heights were distinguished from the cirrus clouds present at about
22 8–9 km altitude, simply by the position of the tropopause except when we could calculate R at
23 1064 nm, because we don't have enough signal-to-noise-ratio to calculate R at 1064 nm in
24 most of the observation period. In each ratio, we observed three peaks above the tropopause
25 height in the analysis period, on 11 June, 23 June, and 6 July. This result suggests that the
26 volcanic aerosol plume circled the Southern Hemisphere three times, a finding that was
27 confirmed by using IASI, Ozone Monitoring Instrument (OMI), and Moderate Resolution
28 Imaging Spectroradiometer (MODIS) satellite data (not shown) (Klüser et al., 2013). To
29 examine the three peaks of the aerosol vertical profiles in greater detail, we calculated the
30 particle depolarization ratio δ_p , to estimate the non-sphericity of the particles:

$$31 \quad \delta_p(z) = \frac{\delta(z)R(z) - \delta_m}{R(z) - 1} \times 100, \quad (5)$$

1 where δ is the total (molecular plus particle) depolarization ratio, calculated with Eq.(3), and
2 δ_m is the depolarization ratio of atmospheric molecules. We used $\delta_m = 0.37\%$ for this lidar
3 system, defined from the spectral transmission data of the interference filter at 532 nm and the
4 Rayleigh backscattering cross sections (Sakai et al., 2003). The measured δ was about 1.0-
5 1.2 % at altitudes higher than about 15 km (see Figs. 4 and 6), and this indicates that δ is sum
6 of δ_m (0.37 %) and the lidar system error (about 0.65 %) where there were no aerosols. We
7 estimated δ_p taking into account of this lidar system error (Sakai et al., 2003). When R is
8 close to 1.0, δ_p has a larger error. For example, when $R=1.05$ and $\delta_p = 8\%$, the error of δ_p is
9 larger than 20 %.

10 We estimated the proportion of non-spherical particles in the volcanic aerosol layers from the
11 particle depolarization ratio over Lauder measured by lidar. On 11 June (Fig. 4(a)), the
12 maximum values of R, δ and δ_p were 26.7 (11.2 km), 16 % (11.8 km) and 19 % (12.0 km),
13 respectively; on 23 June (Fig. 4(b)), they were 18.1 (12.0 km), 25 % (12.3 km) and 32 %
14 (12.4 km), respectively; and on 6 July (Fig. 4(c)), they were 5.3 (11.1 km), 20 % (11.4 km)
15 and 29 % (11.7 km), respectively. Values of δ_p higher than 20 % in the aerosol layer indicate
16 a predominance of non-spherical particles (Sakai et al., 2003). The δ_p values of the PCCVC
17 volcanic aerosol layer were larger than 20 % even on the third overpass during the continuous
18 observation period. By comparison, the δ values of the Eyjafjallajökull volcanic aerosol layers
19 in April 2010 in Iceland were 35–40 % (Ansmann et al., 2010; Gasteiger et al., 2011).
20 According to the analysis by Groß et al. (2012), the wavelength-independent δ_p values of the
21 pure ash layer of the Eyjafjallajökull volcano were between 35 % and 38 %.

22 One interesting feature of the depolarization data warrants further investigation. For each of
23 the three overpass plume observations, δ_p had a local minimum at the backscatter ratio peak.
24 If this is a real physical effect and not an artifact of measurement or retrieval, it suggests some
25 vertical separation of the volcanic plume, for which we have no ready explanation. The
26 centroid height of the volcanic aerosol plumes descended with time after the Pinatubo
27 eruption (Iwasaka et al., 1995) and after the 2008 Kasatochi eruptions in the Aleutian Islands
28 (Bitar et al. 2010). However, because our observation period was brief, we could not tell
29 whether the height of the aerosol plumes was descending.

30

1 3.3 Aerosol optical depth derived from the backscattering ratio

2 Aerosol optical depth (AOD) was calculated as the product of the IBC and S. The time series
3 of the AOD at 532 nm showed three peaks: 0.45 on 11 June, 0.31 on 23 June, and 0.12 on 6
4 July (Fig. 5). As discussed in section 3.2, the presence of three peaks, and the decrease of the
5 peak value with time, is an indication that the volcanic aerosol plume passed over Lauder
6 three times.

7 Because the AOD as calculated in this study depends on the lidar ratio value, the
8 appropriateness of the value chosen for that ratio needs to be considered. According to the
9 analysis (Raman method) of Gro ß et al. (2012), the lidar ratio at 532 nm for the
10 Eyjafjallajökull eruption was 49 ± 5 sr (Maisach, Germany), and according to the analysis of
11 Ansmann et al. (2010), it ranged from 55 ± 5 sr (Maisach) to 60 ± 5 sr (Leipzig, Germany).
12 Hoffmann et al. (2010) reported that the lidar ratio at 532 nm for the Kasatochi eruption event
13 was 65 ± 10 sr. We compared the AODs reported above with AODs calculated by a method
14 that does not use the lidar ratio (Uchino et al., 1983). In this method, the transmission
15 $\tau(z_1, z_2)$, between altitude z_1 and z_2 is

$$16 \quad \tau(z_1, z_2) = \frac{z_2}{z_1} \left[\frac{p(z_2)R(z_1)\beta_m(z_1)}{p(z_1)R(z_2)\beta_m(z_2)} \right]^{1/2}, \quad (6)$$

17 where $p(z)$ is the total received signal photon count at altitude z , $\beta_m(z)$ is the atmospheric
18 molecular backscattering coefficient, and $R(z)$ is the backscattering ratio. The transmission
19 can be determined by choosing two altitudes, z_1 and z_2 , where no aerosols are assumed to
20 exist; therefore, $R(z_1) = R(z_2) = 1$. For example, the AOD on 11 June as determined by this
21 method was 0.52 ± 0.08 ($z_1 = 8.4$ km and $z_2 = 12.0$ km); this AOD value is 13 % larger than
22 the AOD derived from the IBC and S. The values of AOD derived by Eq.(6) are 0.17 and 0.12
23 on 24 June and 6 June, respectively. On average, the AOD derived by IBC was about 20%
24 smaller than AOD derived by Eq.(6). If the lidar ratio is assumed to be 60 sr, AOD will be
25 consistent each other.

26

27

28 4 Discussion

29 The observed PCCVC particle depolarization ratios δ_p were large. On 11 June, the maximum
30 δ_p was 23 %; on 23 June, it was 33 %; and on 6 July, it was 29 %. These large values indicate

1 that the aerosol particles were non-spherical. We then calculated the backscatter-related
2 wavelength exponent A_β as follows:

$$3 \quad A_\beta = -\frac{\ln(\beta_{532}/\beta_{1064})}{\ln(532/1064)}, \quad (7)$$

4 where β_{532} and β_{1064} are the backscattering coefficients at 532 nm and 1064 nm. A_β provides
5 information about the size distribution of both spherical and non-spherical particles that takes
6 account of the complex dependence of backscatter on particle component size, wavelength,
7 and non-sphericity. $A_\beta > 2$ indicates relatively smaller particles (radius $\leq 0.5\mu\text{m}$) and A_β
8 around zero indicates larger particles (radius $\geq 0.5\mu\text{m}$) (Kaufman et al., 1994; Schuster et al.,
9 2006). For background stratospheric aerosols, A_β is about 2.0 (Shibata et al., 1984; Hofmann
10 et al., 2009); for cloud layers A_β is about -0.2 to 0.0 (Kamei et al., 2006; Mona et al., 2012),
11 and for volcanic ash A_β is about 1.0 (Ansmann et al., 2012).

12 Figure 6(a) displays the vertical profiles of R, δ and δ_p at 532 nm, and Fig. 6(b) shows the
13 vertical profiles of R at 532 nm and 1064 nm and of A_β at 532 nm/1064 nm, on 13 June. The
14 peak of R was below the tropopause, but we infer that this represents the volcanic layer
15 because its average A_β at 11–13 km altitude was 0.92, whereas that of the stratospheric
16 background aerosols at 13–15 km was 2.54, and the mean value of cirrus clouds at 8–9.5 km
17 was 1.29×10^{-2} . Although the stratospheric aerosol A_β value at 13–15 km is a little larger
18 than the literature value, the A_β values of the volcanic aerosols and cirrus clouds are
19 consistent with value reported by previous studies (Kamei et al., 2006; Mona et al., 2012;
20 Ansmann et al., 2012). This result indicates that it should be possible to distinguish between a
21 volcanic aerosol layer and underlying cirrus clouds by using the vertical profile of A_β .
22 Unfortunately, because there were optically thick clouds under the volcanic aerosol layers and
23 the vertical backscattering coefficient at 1064 nm were very noisy, we were not able to apply
24 this method to distinguish the aerosols and cirrus clouds on the other days.

25 It is possible to use A_β , δ and δ_p derived from lidar measurement to determine approximately
26 the proportions of sulfur acid aerosols and the ash particles. However, it is not possible to
27 determine the absolute quantity of these particles. Typically, non-spherical and larger particles
28 are volcanic ash, whereas spherical and smaller particles are sulfuric acid aerosols. As
29 mentioned in section 3, the finding that the total and particle depolarization ratios of the

1 PCCVC volcanic aerosols were larger than 20 % suggests that the volcanic plume included
2 many non-spherical and large particles. Therefore, we concluded that the dominant
3 component of the plume observed over Lauder was volcanic ash.

4 Similarly, for aerosols from the eruption of Eyjafjallajökull, the total depolarization ratios
5 were 35–40 % (Ansmann et al., 2010; Gasteiger et al., 2011). In contrast, the Kasatochi ratios
6 were 1.5–5.0 % (Hoffmann et al., 2010) and the ratios for aerosols from the eruption of Nabro
7 volcano in Eritrea in 2011 were $\delta = 1\text{--}2\%$ and $\delta_p = 4\text{--}7\%$ (Uchino et al., 2012). In the case
8 of the eruption of Eyjafjallajökull, Ansmann et al. (2011) reported that sulfate aerosols
9 originating from volcanic SO₂ plumes contributed about 50 % of the particle mass. Miffre et
10 al (2011) used the volcanic ash particle depolarization ratio $\delta = 40 \pm 0.2\%$ obtained from
11 laboratory measurements performed by Muñoz et al. (2004) to determine the composition of
12 the Eyjafjallajökull plume.

13 Recent studies have provided estimates of SO₂ emission from several eruption events.
14 Karagulian et al. (2010) estimated the total mass of SO₂ ejected by the Kasatochi eruption to
15 be 1.7 Tg, based on the IASI high-spectral-resolution infrared radiance measurements.
16 Haywood et al. (2010) estimated that 1.2 Tg of SO₂ was ejected by the Sarychev (Kuril
17 Islands) eruption in June 2009. Clarisse et al. (2012), using IASI data, reported that 1.5 Tg of
18 SO₂ was ejected by the Nabro volcano, and 0.25 Tg by the PCCVC eruption. Because less
19 SO₂ was ejected by the eruption of Puyehue-Cordón Caulle compared with the amounts
20 ejected by the eruptions of Nabro and Kasatochi, the tephra fraction of the PCCVC plume was
21 greater, and its depolarization ratios were larger.

22 We next estimated the influence of the PCCVC volcanic ash particles on the column averaged
23 dry air mole fraction of carbon dioxide (XCO₂) determined by GOSAT. When the GOSAT
24 XCO₂ is retrieved by using the 1.6 μm band without taking account of volcanic ash particles
25 in the upper troposphere and lower stratosphere, the negative bias of XCO₂ is estimated to be
26 2 % for an AOT of 0.4 at 532 nm and surface albedo of 0.28 at Lauder (based on MODIS
27 band2).

28

29 **5 Summary**

30 On 4 June 2011, the Puyehue-Cordón Caulle Volcanic Complex (40.59°S, 72.11°W) in Chile
31 erupted and the volcanic plume passed over Lauder in New Zealand. Because the VAAC at

1 Wellington had forecast that the aerosol plume would pass over New Zealand, we started
2 continuous lidar observations on 11 June. On the same day, we detected the PCCVC volcanic
3 aerosol layer from the profiles of the backscattering ratio R and the depolarization ratio δ at
4 532 nm. This observational result was confirmed by a forward trajectory analysis done by
5 using METEX and some satellite data (from the MODIS, OMI and IASI instruments). We
6 found that the volcanic aerosol layer peak passed over Lauder three times from 11 June to 6
7 July at intervals of 10–12 days. The maximum R value on 11 June, immediately after the
8 eruption, was 26.7 at 11.2km, and the AOD was 0.45. This R value is much larger than the
9 maximum R value of 2.0–3.5 observed at Saga and Tsukuba, Japan, for the Nabro volcano,
10 which erupted on 12 June 2011 (Uchino et al., 2012). On 11 June, when the continuous lidar
11 observation started, the maximum value of δ was 16 % and that of δ_p was 23 %. On 6 July, at
12 the end of the period of continuous lidar observations, the maximum value of δ was 20 %, and
13 that of δ_p was 29 %. Thus, δ_p remained at 20–30 % over the entire observation period, and
14 even one month after the eruption the depolarization ratio had not decreased. This result
15 indicates that the major component of the PCCVC volcanic aerosol layers was non-spherical
16 particles.

17 The backscatter-related wavelength exponent of the PCCVC volcanic aerosols at 1064/532
18 nm was 0.9 at 11–13 km altitude; this value indicates that the PCCVC volcanic aerosols were
19 composed of large particles. According to Ansmann et al. (2012), the wavelength exponents
20 of the Eyjafjallajökull volcanic aerosols were 1.12–1.19. The wavelength exponents of the
21 Kasatochi eruption aerosols were 0.5–1.5 (Tesche et al., 2010). The lidar observations at
22 Lauder showed that the PCCVC volcanic aerosol layers contained non-spherical and larger
23 particles. These results agree with the findings of previous studies, which reported that the
24 volcanic plume of the PCCVC eruption contained less SO_2 than the plumes from the
25 Kasatochi and Nabro eruptions (Karagulian et al., 2010; Clarisse et al., 2012).

26

27 *Acknowledgements*

28 This research was supported in part by the Environment Research and Technology
29 Development Fund (2A-1102) of the Ministry of the Environment, Japan. The author wish to
30 thank the editor.

31

1 **References**

- 2 Alados-Arboledas, L., Olmo, F. J., Ohvri, H. O., Teral, H., Arak, M. and Teral, K.: Evolution
3 of solar radiative effects of Mount Pinatubo at ground level, *Tellus B*, 49, 2, 190-198, 1997.
- 4 Ansmann, A., Tesche, M., Grofl, S., Freudenthaler, V., Seifert, P., Hiebsch, A., Schmidt, J.,
5 Wandinger, U., Mattis, I., Müller, D., and Wiegner, M.: The 16 April 2010 major volcanic
6 ash plume over central Europe: EARLINET lidar and AERONET photometer observations
7 at Leipzig and Munich, Germany, *Geophys. Res. Lett.*, 37, L13 810, doi:
8 10.1029/2010GL043809, 2010.
- 9 Ansmann, A., Tesche, M., Seifert, P., Groß, S., Freudenthaler, V., Apituley, A., Wilson, K.
10 M., Serikov, I., Linnú, H., Heinold, B., Hiebsch, A., Schnell, F., Schmidt, J., Mattis, I.,
11 Wandinger, U., and Wiegner, M.: Ash and fine-mode particle mass profiles from
12 EARLINET-AERONET observations over central Europe after the eruptions of the
13 Eyjafjallajökull volcano in 2010, *J. Geophys. Res.*, 116, D00U02, doi:
14 10.1029/2010JD015567, 2011.
- 15 Ansmann, A., Seifert, P., Tesche, M., and Wandinger, U.: Profiling of fine and coarse particle
16 mass: case studies of Saharan dust and Eyjafjallajökull/Grimsvötn volcanic plumes, *Atmos.*
17 *Chem. Phys.*, 12, 9399–9415, doi: 10.5194/acp-12-9399-2012, 2012.
- 18 [Bernard, A. and Rose, W. I.: The injection of sulfuric acid aerosols in the stratosphere by El](#)
19 [Chichon Volcano and its related hazards to the international air traffic, *Natural Hazards*, 3,](#)
20 [59-67, 1990.](#)
- 21 Bitar, L., Duck, T. J., Kristiansen, N. I., Stohl, A., and Beauchamp, S.: Lidar observations of
22 Kasatochi volcano aerosols in the troposphere and stratosphere, *J. Geophys. Res.*, 115,
23 D00L13, doi: 10.1029/2009JD013650, 2010.
- 24 Bluth, G. J. S., Doiron, S. D., Schnetzler, S. C., Krueger, A. J., and Walter, L. S.: Global
25 tracking of the SO₂ clouds from the June 1991 Mount Pinatubo eruptions, *Geophys. Res.*
26 *Lett.*, 19, 151–154, 1992.
- 27 [Bucholtz, A.: Rayleigh-scattering calculations for the terrestrial atmosphere, *Appl. Opt.* 34,](#)
28 [15, 2765-2773, 1995.](#)
- 29 Clarisse, L., Hurtmans, D., Clerbaux, C., Hadji-Lazaro, J., Ngadi, Y., and Coheur, P.-F.:
30 Retrieval of sulphur dioxide from the infrared atmospheric sounding interferometer (IASI),
31 *Atmos. Meas. Tech.*, 5, 581–594, doi: 10.5194/amt-5-581-2012, 2012.
- 32 Deshler, T.: A review of global stratospheric aerosol: Measurements, importance, life cycle,
33 and stratospheric aerosol, *Atmos. Res.*, 90, pp. 223–232, doi:

1 10.1016/j.atmosres.2008.03.016, 2008.

2 Durant, A. J., Shaw, R. A., Rose, W. I., Mi, Y., and Ernst, G. G. J.: Ice nucleation and
3 overseeding of ice in volcanic clouds, *J. Geophys. Res.*, 113, D09206, doi:
4 10.1029/2007JD009064, 2008.

5 [Dzierma, Y. and Wehrmann H.: On the likelihood of future eruptions in the Chilean Southern](#)
6 [Volcanic Zone: interpreting the past century's eruption record based on statistical analyses,](#)
7 [Andean Geology](#), 39, 3, 380-393, doi: 10.5027/andgeoV39n3-a02, 2012.

8 Fernald, F. G.: Analysis of atmospheric lidar observations: some comments, *Appl. Opt.*, 23, 5,
9 652–653, 1984.

10 Gasteiger, J., Groß, S., Freudenthaler, V., and Wiegner, M.: Volcanic ash from Iceland over
11 Munich: Mass concentration retrieved from ground-based remote sensing measurements,
12 *Atmos. Chem. Phys.*, 11, 2209–2223, doi: 10.5194/acp-11-2209-2011, 2011.

13 Groß, S., Freudenthaler, V., Wiegner, M., Gasteiger, J., Geiß, A., and Schnell, F.: Dual-
14 wavelength linear depolarization ratio of volcanic aerosols: Lidar measurements of the
15 Eyjafjallaökull plume over Maisach, Germany, *Atmos. Environ.*, 48, 85–96, doi:
16 10.1016/j.atmosenv.2011.06.017, 2012.

17 Haywood, J. M. Jones, A., Clarisse, L., Bourassa, A., Barnes, J., Telford, P., Bellouin, N.,
18 Boucher, O., Agnew, P., Clerbaux, C., Coheur, P., Degenstein, D., and Braesicke, P:
19 Observations of the eruption of the Sarychev volcano and simulations using the HadGEM2
20 climate model, *J. Geophys. Res.*, 115, D21 212, doi: 10.1029/2010JD014447, 2010.

21 Hoffmann, A., Ritter, C., Stock, M., Maturilli, M., Eckhardt, S., Herber, A., and Neuber, R.:
22 Lidar measurements of the Kasatochi aerosol plume in August and September 2008 in Ny-
23 Alesund, Spitsbergen, *J. Geophys. Res.*, 115, D00L12, doi: 0.1029/2009JD013039, 2010.

24 Hofmann, D., Barnes, J., O'Neill, M., Trudeau, M., and Neely, R.: Increase in background
25 stratospheric aerosol observed with lidar at Mauna Loa Observatory and Boulder, Colorado,
26 *Geophys. Res. Lett.*, 36, L15 808, doi: 10.1029/2009GL039008, 2009.

27 Iwasaka, Y., Shibata, T., Hayashi, M., Nagatani, M., Ojio, T., Adachi, H., Matsunaga, K.,
28 Osada, K., Mori, I., Fujiwara, M., Akiyoshi, E., Shiraishi, K., Yamazaki, K., Kondoh, K.,
29 and Nakane, H.: Lidar Measurements at Alaska, 1991-1994. Pinatubo Volcanic Effect on
30 Stratospheric Aerosol Layer, *The Review of Laser Engineering*, 23, 2, 166–170, 1995.

31 Kalnay, E., Kanamitsu, M., Kistler, R., Collins, W., Deaven, D., Gandin, L., Iredell, M., Saha,
32 S., White, G., Woollen, J., Zhu, Y., Chelliah, M., Ebisuzaki, W., Higgins, H., Janowiak, J.,
33 Mo, K. C., Ropelewski, C., Wang, J., Leetmaa, A., Reynolds, R., Jenne, R., and Joseph, D.:

1 The NCEP/NCAR 40-Year Reanalysis Project, *Bull. Amer. Meteor. Soc.*, 77, 3, 437–471,
2 1996.

3 Kamei, A., Sugimoto, N., Matsui, I., Shimizu, A., and Shibata, T.: Volcanic aerosol layer
4 observed by shipboard lidar over the tropical western Pacific, *SOLA*, 2, 1–4, 30 doi:
5 10.2151/sola.2006-001, 2006.

6 Karagulian, F., Clarisse, L., Clerbaux, C., Prata, A. J., Hurtmans, D., and Coheur, P. F.:
7 Detection of volcanic SO₂, ash, and H₂SO₄ using the Infrared Atmospheric Sounding
8 Interferometer, *J. Geophys. Res.*, 115, D00L02, doi: 10.1029/2009JD012786, 2010.

9 Kaufman, Y. J., Gitelson, A., Karnieli, A., Ganor, E., Fraser, R. S., Nakajima, T., Mattoo, S.,
10 and Holben, B. N.: Size distribution and scattering phase function of aerosol particles
11 retrieved from sky brightness measurements, *J. Geophys. Res.*, 99, D5, 10 341–10 356, doi:
12 10.1029/94JD00229, 1994.

13 Klüser, L., Erbertseder, T., and Meyer-Arne, J.: Observation of volcanic ash from Puyehue-
14 Cordon Caulle with IASI, *Atmos. Meas. Tech.*, 6, 35–46, doi: 10.5194/amt-6-35-2013, 2013.

15 Lara, L. E., Moreno-Roa, H., and Naranjo, J. A.: Rhyodacitic fissure eruption in Southern
16 Andes (Cordón Caulle; 40.5°S) after the 1960 (Mw:9.5) Chilean earthquake: A structural
17 interpretation, *J. Volcanol. Geoth. Res.*, 138, 127–138, doi:
18 10.1016/j.jvolgeores.2004.06.009, 2004.

19 Latham, T. L., Kumar, P., Nenes, A., Dufek, J., Sokolik, I. N., Trail, M., and Russell, A.:
20 Hygroscopic properties of volcanic ash, *Geophys. Res. Lett.*, 38, 11, L11 802, doi:
21 10.1029/2011GL047298, 2011.

22 McCormick, M. P., L. W. Thomason and C. R. Trepte: Atmospheric effects of Mt. Pinatubo
23 eruption, *Nature*, 373, 399–404, 1995.

24 Miffre, A., David, G., Thomas, B., Abou-Chacra, M., and Rairoux, P.: Interpretation of
25 accurate UV polarization lidar measurements: application to volcanic ash number
26 concentration retrieval, *J. Atmos. Oceanic Technol.*, 29, 558–568, doi: 10.1175/JTECH-D-
27 11-00124.1, 2011.

28 Minnis, P., Harrison, E. F., Stowe, L. L., Gibson, G. G., Denn, F. M., Doelling, D. R., Smith,
29 W. L. Jr.: Radiative climate forcing by the mount pinatubo eruption, *Science*, 259, no.5100,
30 1411-1415, doi: 10.1126/science.259.5100.1411, 1993.

31 Mona, L., Amodeo, A., D'Amico, G., Giunta, A., Madonna, F., and Pappalardo, G.: Multi-
32 wavelength Raman lidar observations of the Eyjafjallajökull volcanic cloud over Potenza,

1 Southern Italy, *Atmos. Chem. Phys.*, 12, 2229–2244, doi: 10.5194/acp-12-2229-2012, 2012.

2 Muñoz, O. M., Volten, H., Hovenier, J. W., Veihelmann, B., van der Zande, W. J., Waters, L.

3 B. F. M., and Rose, W. I.: Scattering matrices of volcanic ash particles of Mount St. Helens,

4 Redoubt, and Mount Spurr volcanoes. *J. Geophys. Res.*, 109, D16201,

5 doi:10.1029/2004JD004684, 2004.

6 Nagai, T., Sakai, T., Uchino, O., Morino, I., Yokota, T. and Liley, B.: Lidar observations of

7 clouds and aerosols over Lauder in the Southern Hemisphere for GOSAT validation,

8 Proceeding of the 46th spring conference of the Remote Sensing Society of Japan, Abstract

9 No. B3, 2009.

10 Nagai, T., Liley, B., Sakai, T., Shibata, T., and Uchino, O.: Post-Pinatubo evolution and

11 subsequent trend of the stratospheric aerosol layer observed by mid-latitude lidars in both

12 Hemispheres, *SOLA*, 6, 69–72, doi: 10.2151/sola.2010-018, 2010.

13 Newhall, C. G. and Self, S.: The volcanic explosivity index (VEI) an estimate of explosive

14 magnitude for historical volcanism, *J. Geophys. Res.*, 87, C2, 1231-1238, doi:

15 10.1029/JC087iC02p01231, 1982.

16 Raga, G. B., Baumgardner, D., Ulke, A. G., Brizuela, M. T., and Kucienska, B.: The

17 environmental impact of the Puyehue-Cordón Caulle 2011 volcanic eruption on Buenos

18 Aires, *Nat. Hazards Earth Syst. Sci.*, 13, 2319–2330, doi: 10.5194/nhess-13-2319-2013,

19 2013.

20 Robock, A.: Volcanic eruptions and climate, *Rev. Geophys.*, 38, 191–219, doi:

21 10.1029/1998RG000054, 2000.

22 Sakai, T., Nagai, T., Nakazato, M., Mano, Y., and Matsumura, T.: Ice clouds and Asian dust

23 studied with lidar measurements of particle extinction-to-backscatter ratio, particle

24 depolarization, and water-vapor mixing ratio over Tsukuba, *Appl. Opt.*, 42, 36, 7103–7116,

25 2003.

26 [Sassen, K.: The polarization lidar technique for cloud research: A review and current](#)

27 [assessment, *Bull. Amer. Meteor. Soc.*, 72, 1848-1866, 1991.](#)

28 Schuster, G. L., Dubovik, O., and Holben, B. N.: Angstrom exponent and bimodal aerosol

29 size distributions, *J. Geophys. Res.*, 111, D07 207, doi: 10.1029/2005JD006328, 2006.

30 Shibata, T., Fujiwara, M., and Hirono, M.: The El Chichon volcanic cloud in the stratosphere:

31 lidar observation at Fukuoka and numerical simulation, *J. Atmos. Terr. Phys.*, 46, 12, 1121–

32 1146, 1984.

1 Solomon, S. Daniel, J. S., Neely III, R. R., Vernier, J.-P., Dutton, E. G. and Thomaso, L.W. :
2 The Persistently Variable "Background" Stratospheric Aerosol Layer and Global Climate
3 Change, *Science*, 33, 866–870, doi: 10.1126/science.1206027, 2011.

4 Tesche, M., Ansmann, A., Hiebsch, A., Mattis, I., Schmidt, J., Seifert, P., and Wandinger, U.:
5 Lidar observations of the Eyjafjallajökull volcanic ash plume at Leipzig, Germany, *Proc.*
6 *SPIE*, 7832, 78 320L–1, doi: 10.1117/12.868516, 2010.

7 Trickl, T., Giehl, H., Jäger, H., and Vogelmann, H.: 35 yr of stratospheric aerosol
8 measurements at Garmisch-Partenkirchen: from Fuego to Eyjafjallajökull, and beyond,
9 *Atmos. Chem. Phys.*, 13, 5205– 5225, doi: 10.5194/acp-13-5205-2013, 2013.

10 Uchino, O., Tokunaga, M., Seki, K., Maeda, M., Naito, K., and Takahashi, K.: Lidar
11 measurement of stratospheric transmission at a wavelength of 340 nm after the eruption of
12 El Chichon, *J. Atmos. Terr. Phys.*, 45, 12, 849–850, 1983.

13 Uchino, O., Nagai, T., Fujimoto, T., Matthews, W. A., and Orange, J.: Extensive lidar
14 observations of the Pinatubo aerosol layers at Tsukuba (36.1°N), Naha (26.2°N), Japan and
15 Lauder (45.0°S), New Zealand, *Geophys. Res. Lett.*, 22, 57–60, doi: 10.1029/94GL02735,
16 1995.

17 Uchino, O., Sakai, T., Nagai, T., Nakamae, K., Morino, I., Arai, K., Okumura, H., Takubo, S.,
18 Kawasaki, T., Mano, Y., Matsunaga, T., and Yokota, T.: On recent (2008–2012)
19 stratospheric aerosols observed by lidar over Japan, *Atmos. Chem. Phys.*, 12, 11 975–11 984,
20 doi: 10.5194/acp-12-11975-2012, 2012.

21 Vernier, J.-P., Thomason, L. W., Pommereau, J.-P., Bourassa, A., Pelon, J., Garnier, A.,
22 Hauchecorne, A., Blanot, L., Trepte, C., Degenstein, D., and Vargas, F.: Major influence of
23 tropical volcanic eruptions on the stratospheric aerosol layer during the last decade, *Geophys.*
24 *Res. Lett.*, 38, 12, L12 807, doi: 10.1029/2011GL047563, 2011.

25 Wiegner, M., Gasteiger, J., Groß, S., Schnell, F., Freudenthaler, V., and Forkel, R.:
26 Characterization of the Eyjafjallajökull ash-plume: potential of lidar remote sensing, *Phys.*
27 *Chem. Earth*, 45-46, 79–86, 2012.

28 [World Meteorological Organization \(WMO\): Definition of the tropopause, WMO Bull., 6,](#)
29 [136, Geneva, Switzerland, 1957.](#)

30 Wu, P.-M., Okada, K., Tanaka, T., Sasaki, T., Nagai, T., Fujimoto, T., and Uchino, O.:
31 Balloon observation of stratospheric aerosols over Tsukuba, Japan Two years after the
32 Pinatubo volcanic eruption, *J. Meteor. Soc. Jpn.*, 72, 475–480, 1994.

33 Zhao, J., Turco, R. P., and Owen, O. B.: A model simulation of Pinatubo volcanic aerosols in

1 the stratosphere, J. Geophys. Res., 100, D4, 7315–7328, doi: 10.1029/94JD03325, 1995.
2

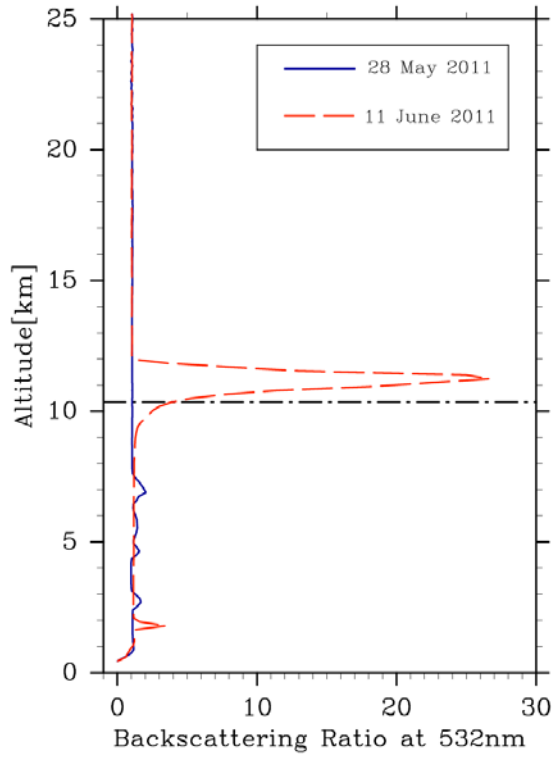
1 **Table 1.** Lidar system at Lauder, New Zealand

2 **System after update (after 18 Feb. 2009)**

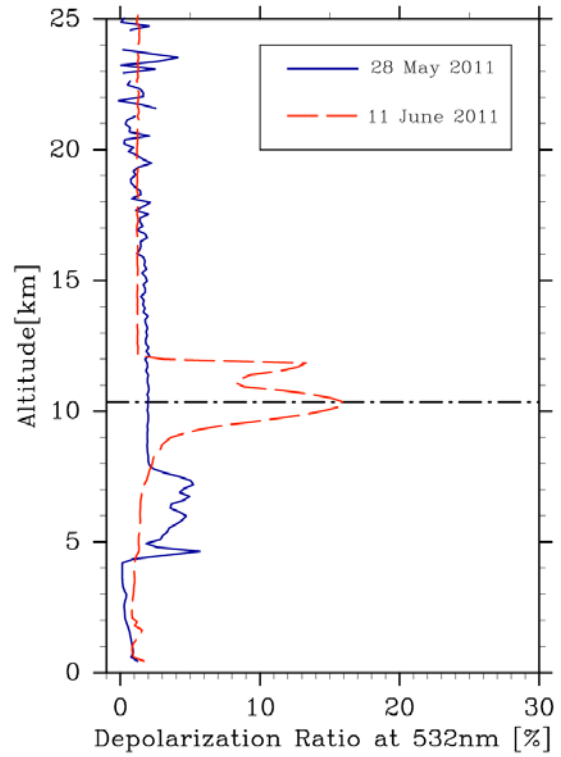
Transmitter		
Laser	Nd:Yag	
Wavelength	532 nm	1064 nm
Pulse Energy	150 mJ	150 mJ
Pulse Repetition	10 Hz	
Beam Divergence	0.2 mrad	
Receiver		
Telescope Type	Ritchey-Chrétien (advanced)	
wavelength	532 nm	1064 nm
Telescope Diameter	30.5 cm (12 inch)	
Field of View (full angle)	1.0 mrad	
Band Width (FWHM)	0.28 nm	0.34 nm
Polarization measurement	Yes	No
Number of Receiving Channel	3	1
Detector	PMT	APD
Signal Processing	12bit A/D + Photon counting	12 bit A/D
Time Resolution	10 seconds (max), 5 minutes (nominal)	
Altitude Resolution	7.5 m	

3

1 (a)



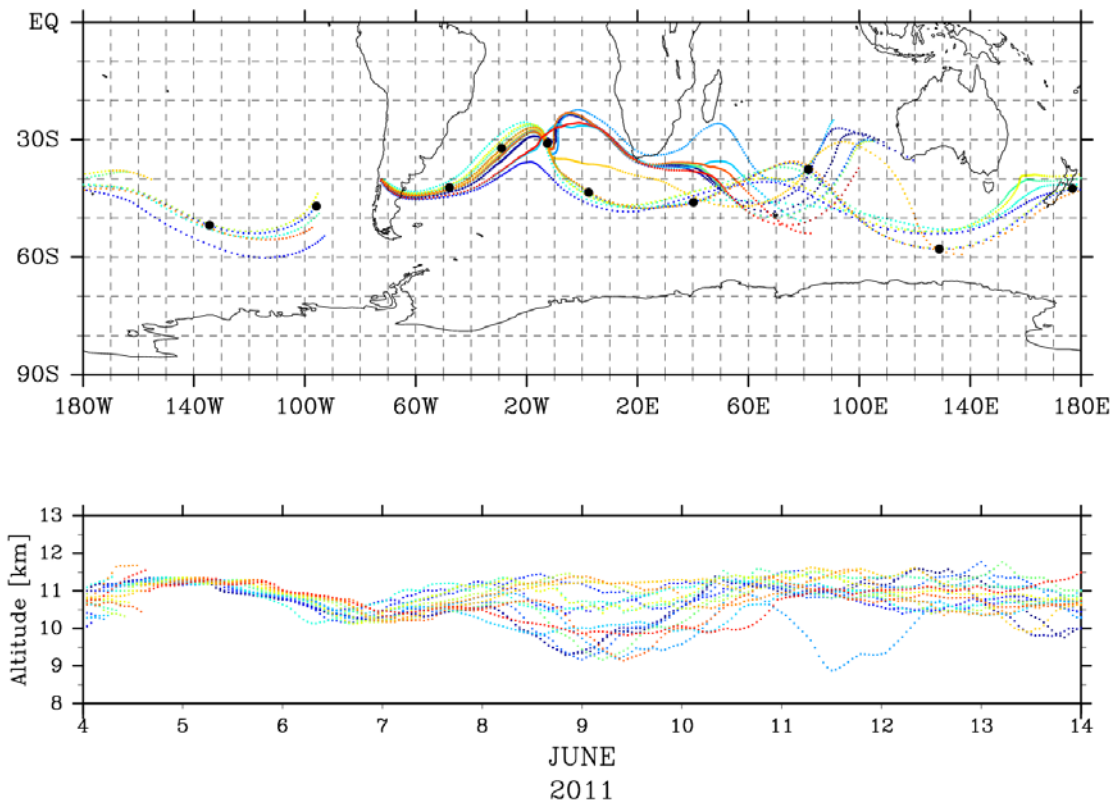
(b)



2
3

4 **Fig. 1.** Vertical profiles of backscattering (left) and depolarization (right) ratios before (28
5 May, blue line) and after (11 June, red line) the PCCVC eruption on 4 June 2011. The
6 horizontal dot-dash line in each panel shows the tropopause height derived from radiosonde
7 data at Invercargill.

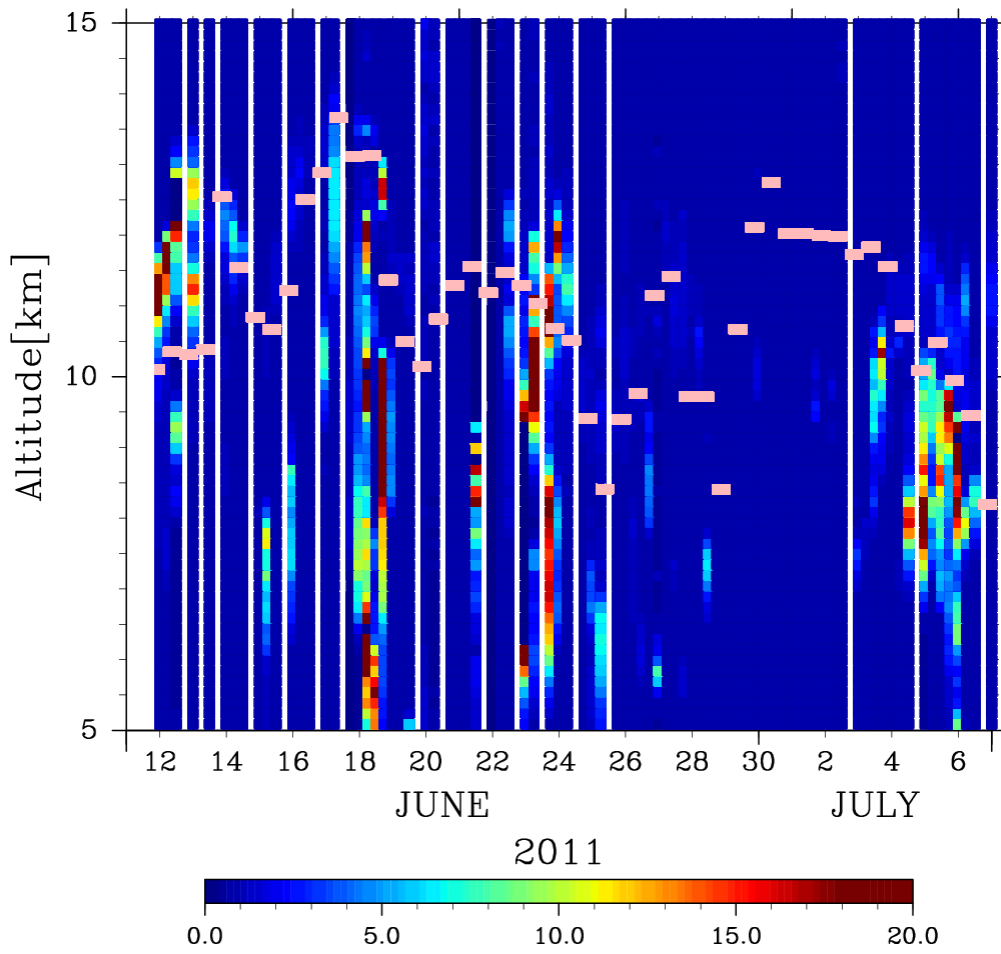
8
9
10



1
 2 **Fig. 2.** Ten-day isentropic forward trajectories of air parcels (colored lines) determined by
 3 using METEX. The starting position was the PCCVC (40.59S, 72.11W), at 11km above the
 4 surface. Large black dots mark each 24-h period in the simulation.

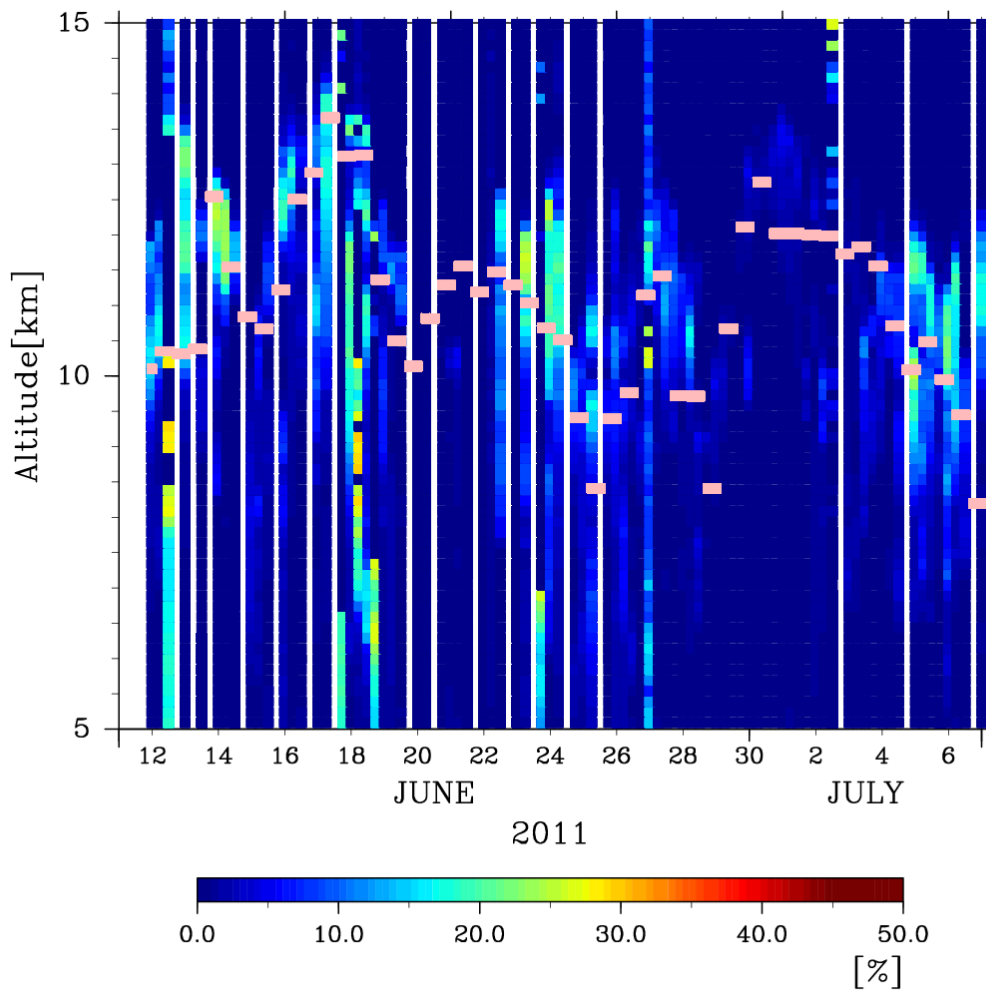
5
 6
 7
 8
 9
 10
 11
 12
 13
 14
 15
 16
 17
 18
 19

1 (a)



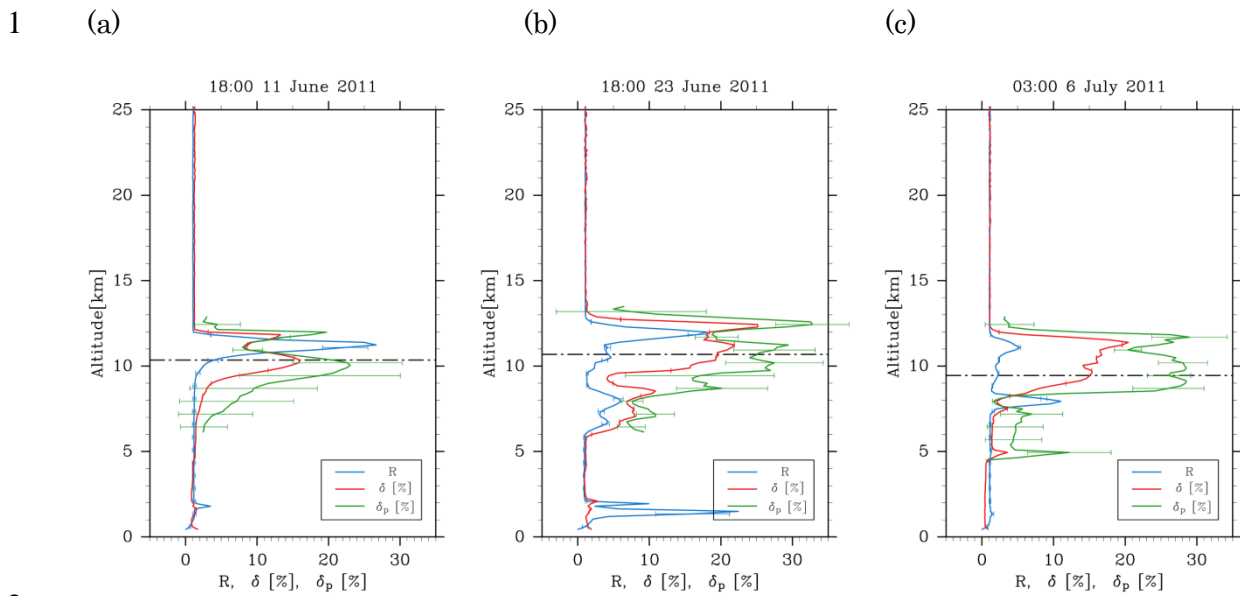
- 2
- 3
- 4
- 5
- 6
- 7
- 8
- 9
- 10
- 11
- 12
- 13
- 14
- 15
- 16

1 (b)



2
3
4
5
6
7
8
9
10
11
12
13
14
15

Fig. 3. Vertical and temporal cross-section of the backscattering ratio (a) and the depolarization ratio (b) at 532 nm. The light purple rectangles show tropopause.



2
3

4 **Fig. 4.** Vertical profiles of the backscattering ratio R (blue line), the total depolarization ratio
5 δ (red line) and the particle depolarization ratio δ_p (green line) observed at on (a) 11 June at
6 18:00LT, (b) 23 June at 18:00LT, and (c) 6 July at 03:00LT. The horizontal dot-dash lines in
7 each panel show tropopause height; (a) 10.3 km, (b) 10.6 km and (c) 9.4 km. The volcanic
8 aerosol layers are indicated by the R , δ and δ_p peaks above the tropopause. **The error bars are**
9 **also show for R , δ , and δ_p profiles.**

10
11
12
13
14
15
16
17
18

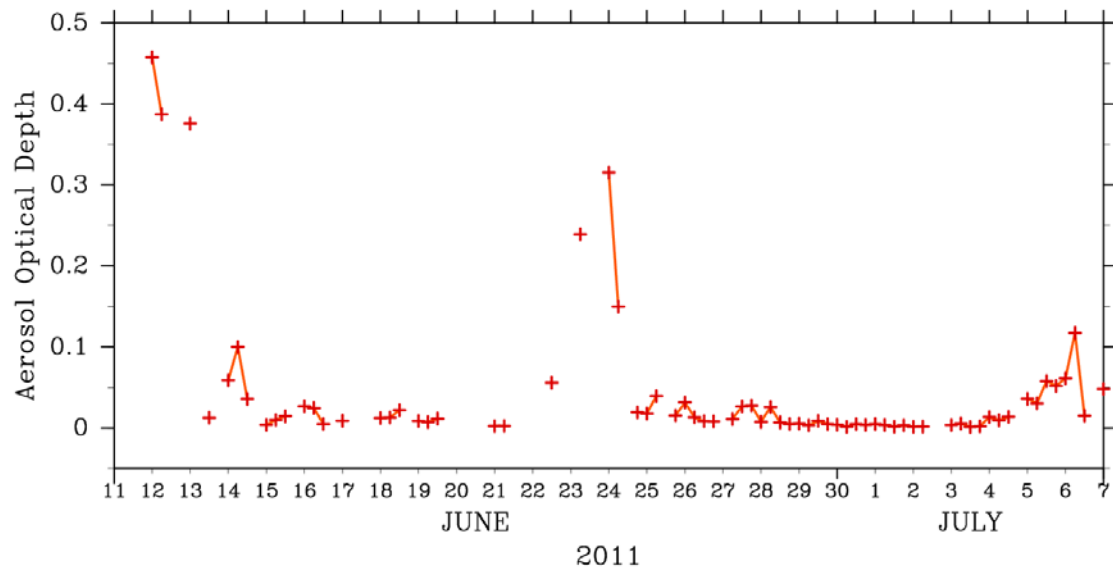
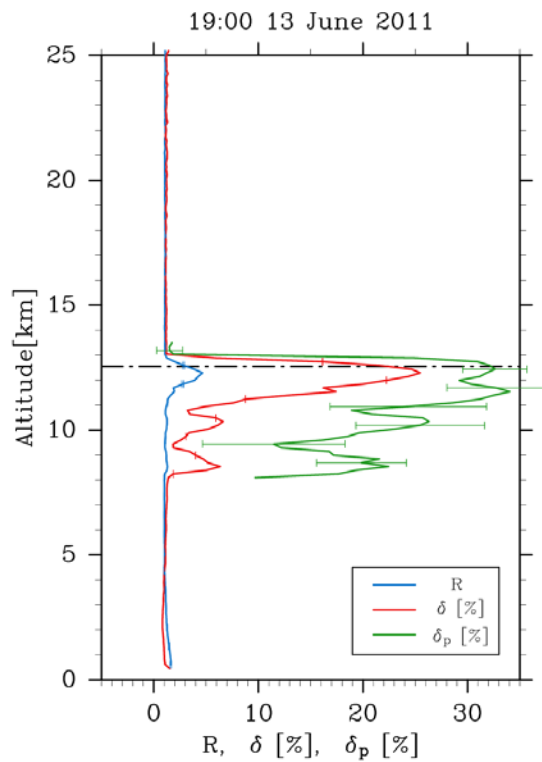


Fig. 5. Temporal variation of the stratospheric AOD over Lauder from 11 June to 6 July 2011. Three AOD peaks occurred of 0.45 on 11 June, 0.31 on 23 June and 0.12 on 6 July.

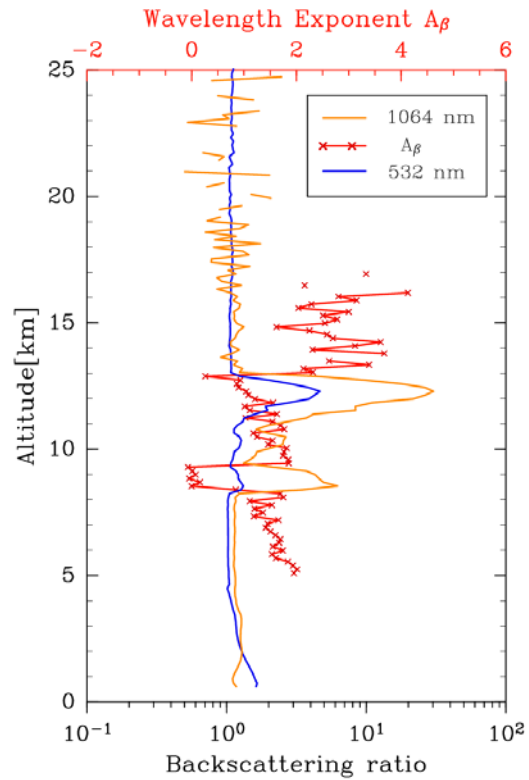
1
2
3
4
5
6
7
8
9
10
11
12
13
14
15
16
17
18
19
20
21
22
23
24

1

(a)



(b)



2

3 **Fig. 6.** (a) Vertical profiles of the backscattering ratio R (blue line), the total depolarization
 4 ratio δ (red line), and the particle depolarization ratio δ_p (green line) at 532 nm on 13 June.
 5 The horizontal dot-dash lines in each panel shows tropopause height. (b) Vertical profiles of
 6 the backscattering ratio at 532 nm (blue line), the backscattering ratio at 1064 nm (orange
 7 line), and the wavelength exponent of the backscattering ratios (A_β) at 1064 nm/532 nm (red
 8 line) on 13 June. The error bars are also show for δ_p profile.